Chemosphere 86 (2012) 1079–1086

Contents lists available at SciVerse ScienceDirect

Chemosphere

journal homepage: www.elsevier.com/locate/chemosphere

Photocatalytic oxidation of monuron in the suspension of WO_3 under the irradiation of UV–visible light

W. Chu *, Y.F. Rao

Department of Civil and Structural Engineering, Research Centre for Urban Environmental Technology and Management, The Hong Kong Polytechnic University, Hung Hom, Kowloon, Hong Kong

ARTICLE INFO

Article history:
Received 17 May 2011
Received in revised form 25 October 2011
Accepted 22 November 2011
Available online 26 December 2011

Keywords:
Monuron
WO_3
Oxidation mechanism
Decay pathway

ABSTRACT

A comprehensive study of the degradation of monuron, one of the phenylurea herbicides, was conducted by UV–Vis/WO_3 process. It was found that hydroxyl radicals played a major role in the decay of monuron while other radicals (*e.g.* superoxide) and hole might also contribute to the decomposition of monuron. The oxidation path likely plays a major role in the generation of hydroxyl radicals. The effects of initial pH level, initial concentration of monuron, and inorganic oxidants on the performance of UV–Vis/WO_3 process were also investigated and optimized. Comparison between monuron decay pathways by UV–Vis/WO_3 and UV/TiO_2 was conducted. The decay mechanisms, including *N*-terminus demethylation, dechlorination and direct hydroxylation on benzene ring, were observed to be involved in the oxidation of monuron in these two processes. Sixteen intermediates were identified during the photodegradation of monuron and degradation pathways were proposed accordingly.

1. Introduction

The application of herbicides is a regular and effective practice to control weed growth. It has been reported that several metric tons of pesticides and herbicides are applied in agricultural activities every year (FAO, 2006). Unfortunately, less than 1% of the total applied herbicides can reach their intended targets, while the dominant majority being disseminated into the aquatic environment via agricultural runoff or leaching (Pimentel, 1995). In addition, their biodegradation process in nature is generally slow (Bobu et al., 2006). Herbicides have thus become some of the most frequently detected micropollutants in natural waters.

Monuron (3-(4-chlorophenyl)-1,1-dimethylurea), a phenylurea derivative has been applied for pre- and post-emergence control of weeds in many crops due to its inhibition of photosynthesis. Phenylurea herbicides are characterized by long life times in the environment, among which monuron has a lifetime of 8 weeks in river waters (Eichelbe and Lichtenb, 1971) and its half-life is around 170 d in the soil (Chu et al., 2007b). Monuron has been reported to be possibly carcinogenic in humans (Ragsdale and Menzer, 1989), and it is suspected of having the potential to become contaminated with dioxins if synthesized under certain conditions (USEPA, 2004). Recently, monuron is banned to use in US (Chu et al., 2007a).

In the past decade, the investigation on visible-light-driven photocatalysts has been one of the most active research areas. Among the semiconductors applied in photocatalysis, TiO_2 has received intensive attention due to its innocuity, low cost and enduring stability. However, TiO_2 is only responsive to UV light owing to its wide band gap. Various TiO_2 catalysts doped with transition metal (Lin et al., 1999; Huang et al., 2006) and nonmetal (Asahi et al., 2001; Tachikawa et al., 2004; Zaleska et al., 2008) or mixed with other metal oxides to form composite semiconductors (Yang et al., 2005; Bian et al., 2008), therefore, have been developed for the degradation of organic pollutants in air and aqueous phase. Whereas some of these photocatalysts have demonstrated sensitivity to visible light, the preparation process of them is mostly time-consuming, expensive and their photocatalytic activities are not sufficient for practical applications. On the other hand, recently tungsten oxide (WO_3) has attracted considerable attention due to the ease of its preparation, long-term stability during irradiation and strong absorption of light in the near UV and luminous regions (Bamwenda and Arakawa, 2001). Most previous studies focus on the application of modified WO_3 such as CuO/WO_3 (Arai et al., 2009), Pt/WO_3 (Kim et al., 2010) and Pd/WO_3 (Arai et al., 2008) as photocatalyst in the decomposition of organic substance. However, the investigation on the degradation mechanism of organic pollutants by sole WO_3-based photocatalysis is still limited.

Several researchers have examined the degradation of monuron in aqueous systems such as direct photolysis by UV irradiation (Chu et al., 2007a), Co/Oxone (Chu et al., 2007b), electro-Fenton (Oturan et al., 2010), ozonation (Tahmasseb et al., 2002) and

* Corresponding author. Tel.: +852 2766 6075; fax: +852 2334 6389.
E-mail address: cewchu@polyu.edu.hk (W. Chu).

0045-6535/$ - see front matter © 2011 Elsevier Ltd. All rights reserved.
doi:10.1016/j.chemosphere.2011.11.062

UV/TiO_2 (Pramauro et al., 1993; Mest'ankova et al., 2005). Different photodegradation intermediates of monuron have also been evaluated by various analytical methods in previous studies (Pramauro et al., 1993; Bobu et al., 2006; Nelieu et al., 2008).

In this study, photocatalytic degradation of monuron in WO_3 suspension under the irradiation of UV–Vis light was investigated. The performance of this system was evaluated in terms of monuron degradation under different conditions such as initial pH level, initial concentration of monuron and the addition of inorganic oxidants. The study on the decay mechanism of monuron was also conducted.

2. Material and methods

Monuron (99%) was obtained from Sigma–Aldrich. The standards of intermediary products 1-4(chlorophenyl)-3-methyl-urea (CPMU) and *p*-chlorophenylurea (*p*-CPU) were purchased from Sigma–Aldrich and Chem Service, respectively. WO_3 powder was prepared from commercial WO_3 (ACROS Organics) as following: the particles of commercial WO_3 were added to DDW (Distilled Deionized Water) under sonication for 40 min to form WO_3 suspension, then the WO_3 suspension was dried by steam to obtain WO_3 powder. The mean diameter of as-prepared WO_3 powder was measured to be 379 nm by Zeta Plus/Zeta Potential Analyzer (Brookhaven Instruments Corporation). The XRD pattern of WO_3 was recorded on a Bruker D8 Advance X-ray diffractometer with Cu Kα radiation (λ = 1.542 Å) at a scan rate of 0.02° 2θ s^{-1}. The accelerating voltage and applied current were 40 kV and 40 mA, respectively. The WO_3 is triclinic as demonstrated in XRD pattern (see Supplementary Materials (SM), Fig. SM-1) in good agreement with the JCPDS 32-1395 standard card. The H_2O_2 was purchased from Riedel-deHaën while potassium iodate (KIO_3) and potassium persulfate ($K_2S_2O_8$) were purchased from International Laboratory. All other chemicals are in analytic purity and all solvents are HPLC grade and used without further purification. The water used in the preparation of all solutions was obtained from a Millipore Waters Milli-Q water purification system.

The photodegradation of monuron was conducted in a computerized Luzchem CCP-4 V photochemical reactor. To ensure a thorough mixing, 150 mL of solution was dispensed into a 300 mL quartz cylinder with mechanical stirring before and during the illumination. Twelve Luzchem LZC-420 lamps were installed in the photoreactor. The experimental installation and the emission spectra of the lamps were stated previously (Rao and Chu, 2010). For UV/TiO_2 photocatalytic reactions, they were conducted in a Rayonet RPR-200 photochemical reactor manufactured by the Southern New England Ultraviolet. Six phosphor-coated low-pressure mercury lamps at 350 nm were installed on the photoreactor. Samples were withdrawn at a predetermined interval and filtered through a 0.2 μm PTFE (Poly Tetra Fluoro Ethylene) membrane to ensure the solution was free from particles prior to quantification. All experiments were carried out at room temperature (air-conditioned) at 23 ± 1 °C in duplicate and the error is less than 5%.

The remaining monuron after reaction was determined by HPLC, which was comprised of a Waters 515 HPLC pump, Waters 2487 Dual λ Absorbance Detector, an Agilent Hypersil ODS column (5 μm, 0.46 × 25 cm), and Waters 717plus Autosampler. The maximum adsorption wavelength (λ_{max}) was selected as 246 nm for monuron. A mixture of 60% acetonitrile and 40% water was used as the mobile phase running at a flow rate of 1 mL min^{-1}. The intermediate compounds whose standards are not available commercially were quantified in terms of ion intensity relative to the initial monuron concentration for comparison.

The identification of intermediates was carried out at an initial monuron concentration of 0.1 mM. A Thermo Quest Finnigan LCQ Duo Mass Spectrometer system was used to identify the reaction intermediates, which consisted of a PDA (Photo Diode Array)-UV detector, and an electrospray ionization with a quadrupole ion-trap mass spectrometer operating at a negative and positive mode. The mobile phase was a mixture of (A) 5 mM ammonia acetate (pH 4.6) and (B) acetonitrile (100%). The composition of the mobile phase was changed according to the following gradient: 95% of A was kept during the first 2 min. From 2 to 26 min, B was steadily increased from 5 to 65%. From 26 to 27 min, B was kept at 65%. Finally, the mobile phase turned to the initial composition until the end of the run.

The chloride, nitrite and nitrate ions generated in the reaction were monitored by the ion chromatography (Dionex Series 4500i) composed of an anion column (Dionex IonPac® AS14 (4 mm × 250 mm), Dionex CD25 Conductivity Detector, and Dionex AS 40 Automated sampler. A mixture of 1 mM of $NaHCO_3$ and 3.5 mM of Na_2CO_3 was used as the mobile phase eluting at 1 mL/min. For the quantification of the ammonium ion produced during the reaction, Dionex IonPac® CS12 (4 mm × 250 mm) was used as a cation column and 0.022 M methane sulfonic acid was used as the mobile phase eluting at 1 mL min^{-1}. The total organic carbon (TOC) was analyzed by a Shimadzu TOC-5000A analyzer equipped with an ASI-5000A autosampler to determine the mineralization of the organic pollutants during this process.

A HPLC technique was utilized to evaluate the production of hydroxyl radicals. Salicylic acid (SA) was used as a selective trapping reagent of hydroxyl radical. The concentration of the three resulting products, i.e., 2,3-dihydroxybenzoic acid (2,3-DHBA), 2,5-dihydroxybenzoic acid (2,5-DHBA) and catechol, were measured by HPLC and the sum of the three concentrations was used to quantify the generation of hydroxyl radical in the applied processes (Diez et al., 2001).

3. Results and discussion

3.1. Photodegradation of monuron and effects of various scavengers on monuron degradation

The photodegradation of monuron in WO_3 suspension is illustrated in Fig. 1. More than 90% of monuron with an initial concentration of 0.025 mM was decomposed in 3 h, while no monuron decay was observed by the sole-irradiation (420 nm) in the absence of WO_3 (data not shown). As a comparison, the decay of

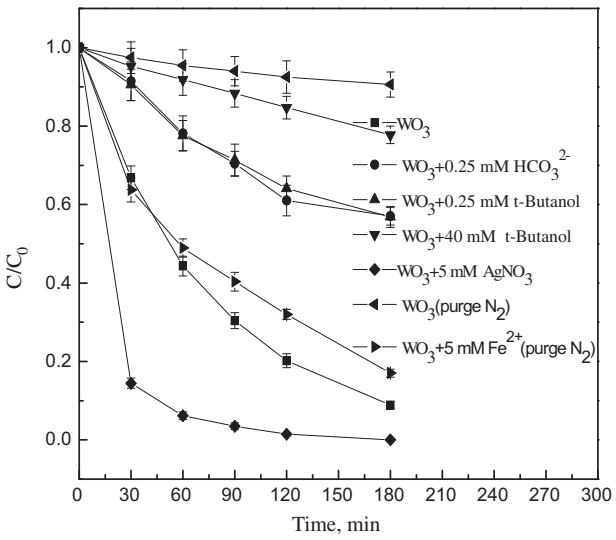

Fig. 1. Effect of radical scavengers and electron scavengers. (*Note*: the initial concentration of monuron is 0.025 mM, initial pH is 6 and WO_3 dosage is 0.3 g L^{-1}.)

monuron in TiO_2 (P25) under the irradiation of UV–Vis light was also investigated. After 3 h of irradiation, only around 24% of monuron was removed (data not shown), indicating UV–Vis/WO_3 system is much more effective than UV–Vis/TiO_2 system in terms of monuron degradation. To understand the photodegradation mechanism of monuron in this process, the effects of various radical scavengers and electron scavengers on the performance of this process were investigated. As also indicated in Fig. 1, the presence of 0.25 mM HCO_3^- or tert-butanol noticeably retarded the degradation of monuron, where higher the concentration of tert-butanol greater the reduction of the degradation rate. This indicates hydroxyl radicals are principally responsible of the decomposition of monuron since bicarbonate and tert-butanol selectively quench hydroxyl radicals. The photocatalytic production of HO· on WO_3 surface may theoretically result from either a reductive path (Eqs. (1) and (2)) or an oxidative path (Eq. (3)) (Kim et al., 2010). It's interesting to note that the decay of monuron was drastically inhibited under anaerobic condition (by purging N_2 gas) suggesting the presence of O_2 (dissolved oxygen) plays an important role in the generation of HO· via the reductive path (Eq. (2)) or in the prevention of the recombination of electrons and holes (Eq. (1)). Under anaerobic condition, if hydroxyl radicals were generated through the reductive path, the decay of monuron would be significantly inhibited even in the presence of other electron scavengers. However, more than 83% removal of monuron was achieved (in 3 h) when 5 mM Fe^{3+} was added to the system as a sole electron acceptor (taking the role of O_2 to quench the electron in Eq. (1)) in the absence of O_2, indicating the production of HO· through the reductive path is minor (Eq. (2)). The generation of HO· mainly through the oxidative path was confirmed by a separate test, where the addition of another electron acceptor 5 mM $AgNO_3$ significantly accelerated the decay rate of monuron, especially in the first 30 min with more than 85% removal of monuron achieved (compared to around 33% removal without the presence of 5 mM $AgNO_3$). It was also observed that even at the high tert-butanol concentration of 40 mM, around 23% reduction of monuron was still achieved and the addition of 0.25 mM KI significantly inhibited monuron degradation (falling from 91% to 9%, data are not shown), implying other radicals such as superoxide and hole may also contribute to monuron's decay since tert-butanol is a weak scavenger of VB holes while I^- is an effective hole scavenger.

$$2e^-_{CB} + O_2 + 2H^+ \rightarrow H_2O_2 \quad (1)$$

$$H_2O_2 + e^-_{CB} \rightarrow OH^- + HO^\cdot \quad (2)$$

$$h^+_{VB} + H_2O \text{ (or } OH^-) \rightarrow HO^\cdot \quad (3)$$

3.2. Effect of the initial concentration of monuron

The concentration of herbicides in waters from various sources may range considerably, which makes the investigation on the effect of initial monuron concentration critical for the real application. The decay rate of monuron was tested with varied initial concentrations as shown in Fig. 2. The decay of monuron in this system was found to follow pseudo first-order kinetics within the tested range. As also demonstrated in Fig. 2, higher initial monuron concentration results in lower decay rate under the same reaction conditions.

It was known that the Langmuir–Hinshelwood (LH) kinetics can be used to quantitatively delineate surface reactions in heterogeneous photocatalysis systems assuming the homogeneous reaction is insignificant (Fox and Dulay, 1993). The initial rate, r_0, can be expressed as:

$$r_0 = -\frac{dC_0}{dt} = \frac{kKC_0}{1 + KC_0} \quad (4)$$

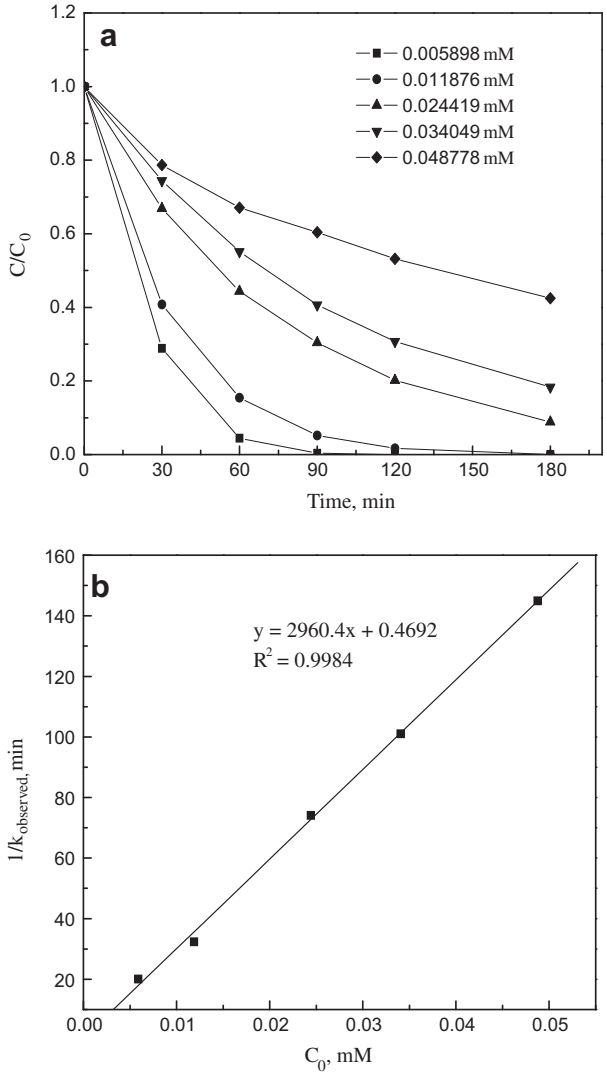

Fig. 2. (a) Monuron degradation at different initial concentration. (b) $1/k_{observed}$ vs C_0 (*Note*: WO_3 dosage is 0.3 g L^{-1} and initial pH is 6.)

where C is the concentration of monuron at time t, C_0 is the initial concentration of monuron, K is the equilibrium absorption constant of monuron on the surface of catalyst WO_3 (mM^{-1}) and k represents the limiting reaction rate at maximum coverage in this system (mM min^{-1}).

For pseudo first-order kinetics, the incorporation of $-dC_0/dt = k_{observed}\, C_0$ (*i.e.* initial condition) into Eq. (4) gives:

$$k_{observed}C_0 = \frac{kKC_0}{1 + KC_0} \quad (5)$$

The linearization of Eq. (5) gives

$$\frac{1}{k_{observed}} = \frac{1}{k}C_0 + \frac{1}{kK} \quad (6)$$

with an intercept of $1/kK$ and slope of $1/k$. $1/k_{observed}$ vs C_0 was plotted in Fig. 2b. The degradation of monuron at various initial concentrations fits well to the LH model with a linear regression (r^2) of 0.9984. The two constants, k and K, were calculated to be 3.38×10^{-4} mM min^{-1} and 6309 mM^{-1} from the slope and intercept, respectively.

3.3. Effect of initial pH level

Initial pH level plays an important role in the performance of TiO_2-based photocatalytic process according to previous studies (Choy and Chu, 2005; Bansal et al., 2010; Elsellami et al., 2010). The investigation on the photocatalytic activity of WO_3 at different pH values, however, is very limited. The effect of initial pH on monuron decomposition was thus examined with initial concentration of monuron fixed at 0.025 mM. The degradation of monuron can be described by pseudo first-order kinetics at different pH levels, and the observed rate constants are summarized in Fig. 3. The pH level of the suspension was quite stable during the degradation reaction of monuron with initial pH at 3.06 while the pH level of the suspension declined during 3 h of the reaction with initial pH at other levels (data not shown). Under acidic (pH 3.06) and basic conditions (pH 7.76 and 9.8), monuron degradation rate was significantly retarded and an optimal pH was found at 6 as illustrated in Fig. 3b. The point of zero charge of WO_3 was reported to be around pH 2.5 (Anik and Cansizoglu, 2006), at which zeta potential is zero, indicating WO_3 particles would display lowest colloid stability in the vicinity of pH 2.5. The low colloid stability could lead to the aggregation and larger hydrodynamic diameter of WO_3 particles. To verify this, the hydrodynamic diameter of WO_3 particles was measured to be 798, 379, and 247 nm at pH level of 3.06, 6.0, and 9.8, respectively. The aggregation of WO_3 particles caused a loss in the effective surface area and consequently a decrease in the photocatalytic activity of photocatalyst. Similar phenomena have been observed by other researchers (Li et al., 2010; Mogyorosi et al., 2010). It was reported that tungsten oxide could be dissolved when pH value is higher than 6 due to its acidic property (Freedman, 1960), which may rationalize the low photocatalytic activity of WO_3 under basic condition. In order to justify this point, the recovery rate was investigated after WO_3 particles were suspended in DDW at different pH levels for 3 h. The recovery efficiency of WO_3 at pH 9.8 (80%) is noticeably lower than that at pH 3.0 (91%) and 6.0 (95%), which confirms the above statement. However, it is interesting to note that as 80% recovery efficiency was observed at pH 9.8, about 0.24 g L^{-1} WO_3 still remained in the solution stoichiometrically. As shown in Fig. SM-2 (pH ~ 6), the $k_{observed}$ at the dosage of 0.2 g L^{-1} is 0.0078 min^{-1} which is much higher than that at pH 9.8 (0.003 min^{-1} in Fig. 3), implying another factor other than the dissolution should account for the additional low-photocatalytic-activity of WO_3 under basic condition. The WO_3 carries negative charges under basic condition since its pzc (point of zero charge) is around 2.5, while the pK_a of monuron was reported to be 4.64 ± 0.07, which makes the monuron molecule carrying negative charge when pH level is higher than 4.64. As a result, the negative charges on the surface of WO_3 may hamper the adsorption of negatively-charged monuron to its surface due to electrostatic repulsion and therefore, the lower reaction rate was observed.

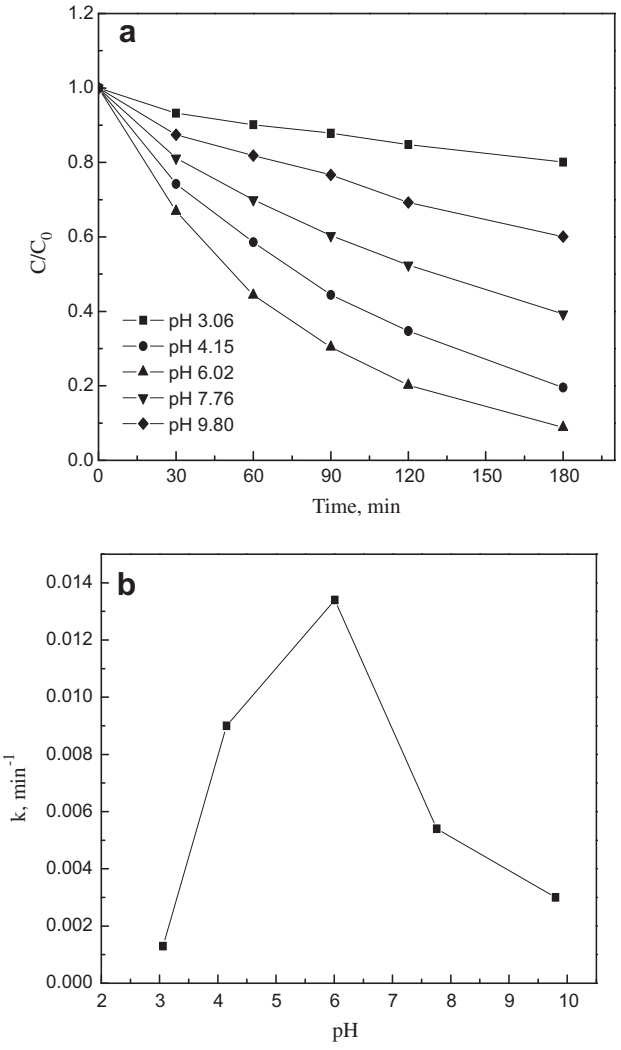

Fig. 3. (a) Monuron degradation at various pH levels. (b) $k_{observed}$ vs pH value (*Note*: the initial concentration of monuron is 0.025 mM and WO_3 dosage is 0.3 g L^{-1}.)

3.4. Effect of inorganic oxidants

It has been reported that the inorganic oxidants such as IO_3^-, BrO_3^-, H_2O_2, $S_2O_8^{2-}$ can be used as additives to improve the performance of UV/TiO_2 process by scavenging electrons on the conduction band or offering additional reactive radicals (Wang and Hong, 1999; Choy and Chu, 2007; Selvam et al., 2007). Whether or not the inorganic oxidants may influence the photodegradation rate of organic compounds in WO_3 suspension under the irradiation of UV–visible light, however, still remains unanswered. Iodate, hydrogen peroxide and persulfate were therefore selected as probes in this study. As illustrated in Fig. 4a, H_2O_2 and $S_2O_8^{2-}$ significantly enhance the decay rate of monuron while IO_3^- shows no influence on the degradation of monuron. The $S_2O_8^{2-}$ and H_2O_2 may act as electron acceptor to prevent the recombination of electron and hole and simultaneously become the sources to offer additional hydroxyl radicals (Eqs. (7) and (8)) and sulfate radicals (Eqs. (9) and (10)).

$$H_2O_2 + e_{CB} \rightarrow OH^- + HO^{\cdot} \quad (7)$$

$$H_2O_2 + O_2^{\cdot-} \rightarrow OH^- + HO^{\cdot} + O_2 \quad (8)$$

$$S_2O_8^{2-} + e_{CB} \rightarrow SO_4^{\cdot-} + SO_4^{2-} \quad (9)$$

$$SO_4^{\cdot-} + H_2O \rightarrow HO^{\cdot} + SO_4^{2-} + H^+ \quad (10)$$

On the other hand, one-electron reduction of IO_3^- may not match the conduction band level of WO_3 (around 0.37 V vs NHE) (Scaife, 1980), IO_3^-, thus, could not act as electron-acceptor in this reaction.

The generation of hydroxyl radicals has also been evaluated in WO_3/UV–Vis, WO_3/H_2O_2/UV–Vis, WO_3/IO_3^-/UV–Vis and WO_3/$S_2O_8^{2-}$/UV–Vis processes. The sum of the concentrations of 2,3-DHBA, 2,5-DHBA and catechol was used to quantify the production of hydroxyl radical when SA was used as a scavenger of hydroxyl radicals. The addition of H_2O_2 significantly increased the yield of hydroxyl radicals (see Fig. 4b) while the presence of IO_3^- gave no beneficial effect on the production of hydroxyl radicals. Furthermore, it is interesting to observe that no 2,3-DHBA, 2,5-DHBA

and catechol were detected in $WO_3/S_2O_8^{2-}$/UV–Vis process. It may be because the decay rate of these three intermediates is much faster than that of SA. In an independent test, the $k_{observed}$ of 2,3-DHBA, 2,5-DHBA and catechol degradation was found to be around 2, 3, and 3.6 times faster than that of SA under the same conditions. Even in the sole-$S_2O_8^{2-}$ process (*i.e.* without WO_3 nor irradiation of visible light), around 30% of 2,5-DHBA (at 0.1 mM) was decayed in 2 h, while no degradation of SA was observed at all.

3.5. Comparison between photocatalytic decay pathways of monuron by UV–Vis/WO_3 and UV/TiO_2

It is believed that hydroxyl radicals play a key role in the decomposition of organic compounds by UV/TiO_2 process. The investigation on the transformation products of monuron produced both in UV–Vis/WO_3 and UV/TiO_2 processes may shed a bright light on the degradation mechanism of monuron by UV–Vis/WO_3 process. The same concentration of monuron (0.1 mM) was degraded under the irradiation of UV or UV–Vis light, where 16 intermediates were identified during these two processes on the basis of the molecular ions and mass fragment ions detected by MS spectrum. The information of the intermediates including the mass of deprotonated ion ($[M-H]^+$) and protonated ion ($[M+H^+]$), the proposed molecular structure, and retention time is summarized (see Table 1, Supplementary Materials). As shown in Table 1 (Supplementary Materials) and Fig. SM-3, compound 1 was not detected in the UV/TiO_2 process while compound 3 was not identified in UV–Vis/WO_3 process. In addition, $[M+acetate]^-$ ions were detected as a base peak of the mass spectra for most intermediates and monuron due to 5 mM ammonium acetate being used as mobile phase when the negative-ion mode was employed in this study (Barcelo and Albaiges, 1989). The evolution profiles of major intermediates in these two processes were organized and shown in Fig. 5a and b (trace intermediates not included). As indicated in Fig. 5, the yield of compound 16 is the highest in both processes. Fig. 5 also shows the yield of compound 11 (CPMU) is second highest during monuron decay by UV–Vis/WO_3 process while its yield is quite low in UV/TiO_2 process (Fig. SM-3 also demonstrates a clear picture). This may be because CPMU suffers fast decomposition in UV/TiO_2 process. The formation/degradation profiles of other products generated during these two processes are quite similar. It was also found that the decay of monuron was involved with *N*-demethylation through alkylic-oxidation, dechlorination (hydroxylation at the chlorine site), and

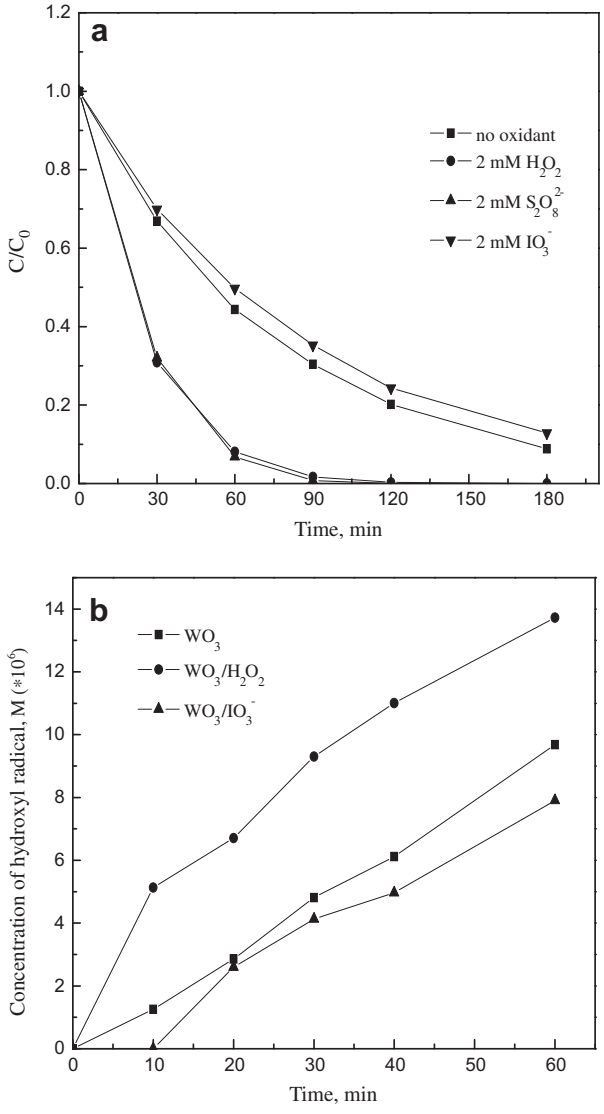

Fig. 4. (a) Effect of various inorganic oxidants. (b) Concentration of hydroxyl radical under different conditions (*Note*: the initial concentration of monuron is 0.025 mM, initial pH is 6 and WO_3 dosage is 0.3 g L^{-1}.)

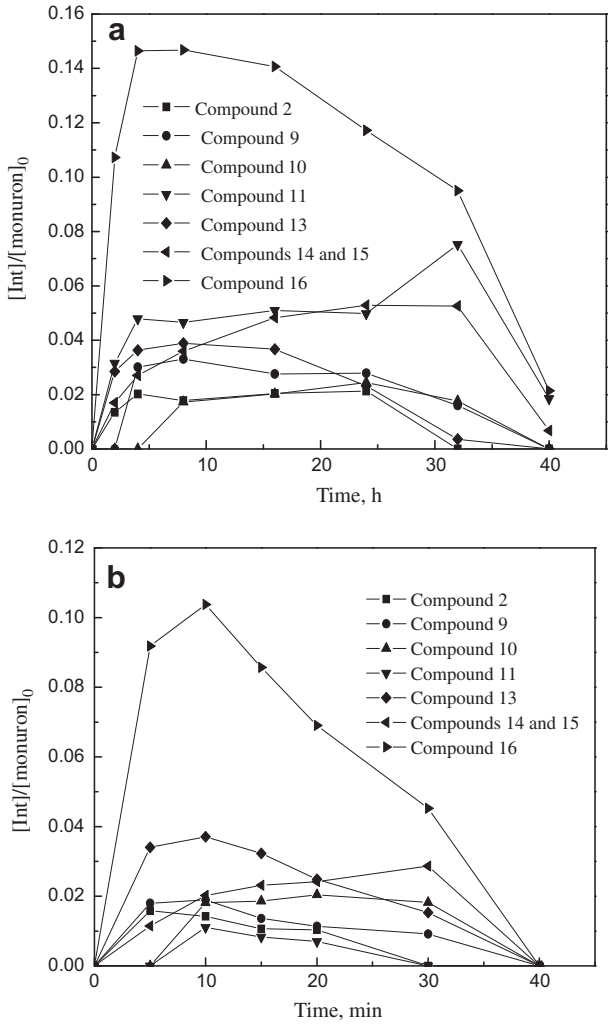

Fig. 5. (a) Evolution profile of intermediates generated in UV–Vis/WO_3 system. (b) Evolution profile of intermediates produced in UV/TiO_2 system (*Note*: the initial concentration of monuron is 0.1 mM, initial pH is 6 and WO_3 dosage is 0.3 g L^{-1}; for UV/TiO_2 system, TiO_2 dosage is 0.2 g L^{-1}.)

hydroxylation of the benzene ring in both processes. Compared to previous studies involved in other advanced oxidation processes (AOPs), more intermediates were identified during the treatment of monuron in this contribution. During monuron degradation by Fe^{3+}/UV (Mest'ankova et al., 2004), only five main intermediates were detected (compounds 10, 11, 13, 16 and 1-(4-chlorophenyl)-3-hydroxylmethyl-3-methylurea). Three intermediates (compounds 11, 16 and 1-(4-hydroxylphenyl)-3,3-dimethylurea) were identified during the treatment of monuron by ozonation (Tahmasseb et al., 2002). It was reported that 1-(4-chlorophenyl)-3-hydroxyl methylurea (compound 8), 1-(4-chlorophenyl)-3-methylurea (compound 11), 4-chlorophenylurea (compound 9), 4-chloroaniline, 4-chlorophenylisocyanate and hydroquinone were detected during monuron degradation by UV/TiO_2 or photo-Fenton process (Bobu et al., 2006). In their study, 4-chloroaniline, 4-chlorophenylisocyanate and hydroquinone were identified by GC-MS.

Therefore, the degradation pathways of monuron by UV–Vis/WO_3 and UV/TiO_2 processes were proposed on the basis of the profile analysis as illustrated in Fig. 6. The decomposition of monuron was initiated by the attack of $HO^{\cdot}$ on the chlorine site of the benzene ring, and *N*-terminus methyl leading to the generation of compounds 2, 13 and 16, respectively at the first step. The emergence of compound 2 was accompanied by the release of chlorine at the beginning of the reaction, which has been confirmed by the detection of chloride ion in the solution. Based on the yield of these three intermediates, the oxidation of *N*-terminus methyl group should play a major part in the degradation of monuron due to the highest yield of compound 16. However, it should be noted around 14% chlorine was released during the first 2 h of reaction (data not shown), suggesting dechlorination (hydroxylation at the chlorine site on the benzene ring) also make an important contribution to the decomposition of monuron. The demethylation of compound 2 resulted in the production of compound 1. Compound 7 came from the oxidation of compound 13. The further oxidation and demethylation of *N*-terminus formaldehyde group of compound 16 led to the generation of compound 14 and compound 11 (CPMU). Compounds 8, 1 and 10 are believed to come from the oxidation of *N*-terminus methyl group, dechlorination-hydroxylation and direct hydroxylation on the benzene ring (without dechlorination) of compound 11 (CPMU), respectively. These pathways were confirmed by an individual test using the compound 11 (CPMU) as the initial probe in UV–Vis/WO_3 process. It is interesting to note the yield of compound 1 is quite low although both the dechlorination–hydroxylation of compound 11 and demethylation of compound 2 could generate compound 1.

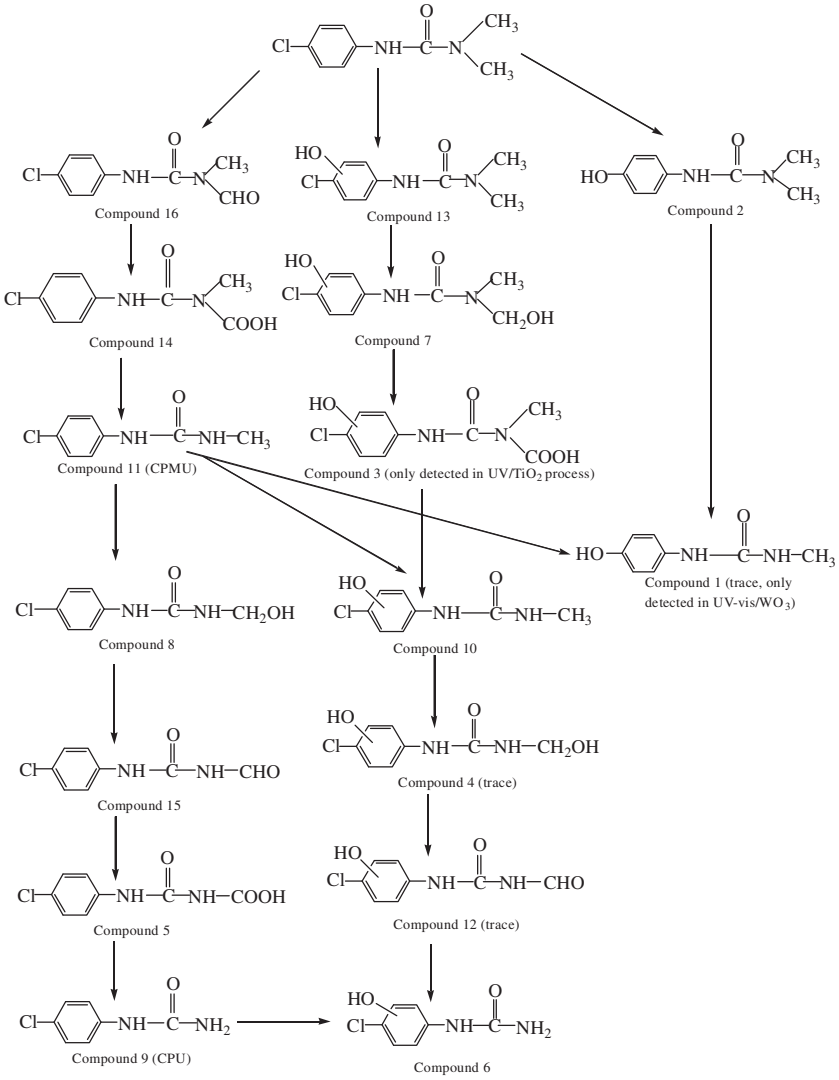

Fig. 6. Degradation pathways of monuron for both UV–Vis/WO_3 and UV/TiO_2 processes.

Compound 1 was even not detected during monuron degradation by UV/TiO_2 process. The intermediates from dechlorination–hydroxylation pathway may be more susceptible to the attack of radicals than compounds containing chlorine due to the electron-withdrawing property of chlorine. The compound 1, thus, could not accumulate to a high concentration. The further *N*-terminus oxidation of compound 8 generates compounds 15 and 5. The decarboxylation of compound 5 produces compound 9 (CPU). Compound 11 may not be the only source contributed to the production of compound 10. Compound 10 may also result from the oxidation and decarboxylation of compound 7 via compound 3 which was identified in UV/TiO_2 process. The *N*-terminus oxidation of compound 10 caused the generation of compounds 4 and 12. The oxidation and decarboxylation of compound 12 can produce compound 6. Compound 6 may also come from the hydroxylation of the benzene ring of compound 9, which was confirmed by an additional test using the compound 9 (CPU) as the initial probe compound in this reaction.

All intermediates were categorized into alkylic-oxidation derivatives (AODs), dechlorination-hydroxylation derivatives (DHDs), and derivatives from the hydroxylation of benzene ring (HBDs). To elucidate the major decay pathway involved in these two processes, the transformation of monuron, intermediates (in terms of AODs, DHDs and HBDs) and the mass balance of benzene ring were reorganized and incorporated in Fig. 7a and b. The concentration of AODs is much higher than that of DHDs and HBDs, indicating the degradation of monuron via alkylic-oxidation is a priority decay pathway in both UV–Vis/WO_3 and UV/TiO_2 processes. This can be rationalized as following: the substitution of the phenyl ring by chlorine atoms lowers its susceptibility towards any electrophilic or radical attack due to electron-drawing property of chlorine leading to the lower electron density on the benzene ring, resulting in the attack on the urea N-terminus group more competitive.

The evolution of chloride, ammonium, nitrate and TOC was also monitored during the monuron decay reaction by UV–Vis/WO_3 process (data are not shown). Around 90% chlorine was released as chloride ion while only trace nitrate and no ammonium ion was detected at the end of the reaction. Judging from the mass balance of benzene ring in Fig. 7a, the cleavage of benzene ring occurred during the degradation of monuron, however, the TOC removal is insignificant. This suggests most aromatic compounds were ring-opened into simple aliphatic acids, which contributes to the TOC in the solution.

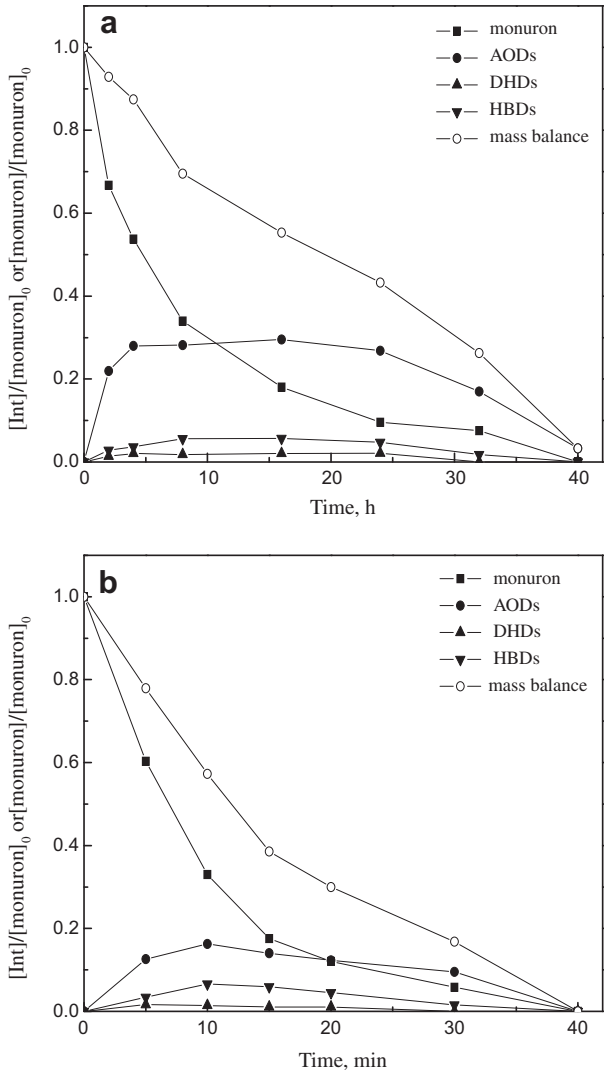

Fig. 7. (a) Process summary of UV–Vis/WO_3 (where [Int] stands for the concentration of intermediates); (b) Process summary of UV/TiO_2 (where [Int] stands for the concentration of intermediates).

4. Conclusions

Hydroxyl radicals are believed to play a major role in the decomposition of monuron in UV–Vis/WO_3 system, judging from monuron decay being significantly hampered after the application of hydroxyl radical scavengers as well as the comparison of generated intermediates and decay mechanism between UV–Vis/WO_3 and UV/TiO_2 processes. The generation of hydroxyl radicals mainly proceeds through the oxidation path. The influence of initial pH value, initial concentration of monuron and inorganic oxidants on the decay rate of monuron has also been investigated. The optimal pH level for the WO_3-based photocatalysis under UV–Vis light was found to be 6.0. Hydrogen peroxide and persulfate were observed to exert a positive influence on the performance of UV–Vis/WO_3 system while iodate did not show any appreciable influence on the decay rate of monuron in this system. It is convincing that UV–Vis/WO_3 process is cost efficient and practically applicable in the removal of persistent organic compounds in natural waters since it can work under the irradiation of near UV and visible light.

Acknowledgment

The authors gratefully acknowledge the financial support from the Hong Kong Polytechnic University (GU-709).

Appendix A. Supplementary material

Supplementary data associated with this article can be found, in the online version, at doi:10.1016/j.chemosphere.2011.11.062.

References

Anik, M., Cansizoglu, T., 2006. Dissolution kinetics of WO_3 in acidic solutions. J. Appl. Electrochem. 36, 603–608.

Arai, T., Horiguchi, M., Yanagida, M., Gunji, T., Sugihara, H., Sayama, K., 2008. Complete oxidation of acetaldehyde and toluene over a Pd/WO_3 photocatalyst under fluorescent- or visible-light irradiation. Chem. Commun., 5565–5567.

Arai, T., Horiguchi, M., Yanagida, M., Gunji, T., Sugihara, H., Sayama, K., 2009. Reaction mechanism and activity of WO_3-catalyzed photodegradation of organic substances promoted by a CuO cocatalyst. J. Phys. Chem. C 113, 6602–6609.

Asahi, R., Morikawa, T., Ohwaki, T., Aoki, K., Taga, Y., 2001. Visible-light photocatalysis in nitrogen-doped titanium oxides. Science 293, 269–271.

Bamwenda, G.R., Arakawa, H., 2001. The visible light induced photocatalytic activity of tungsten trioxide powders. Appl. Catal. A – Gen. 210, 181–191.

Bansal, P., Singh, D., Sud, D., 2010. Photocatalytic degradation of azo dye in aqueous TiO_2 suspension: Reaction pathway and identification of intermediates products by LC/MS. Sep. Purif. Technol. 72, 357–365.

Barcelo, D., Albaiges, J., 1989. Characterization of organo-phosphorus compounds and phenylurea herbicides by positive and negative-ion thermospray and liquid-chromatography mass-spectrometry. J. Chromatogr. 474, 163–173.

Bian, Z.F., Zhu, J., Wang, S.H., Cao, Y., Qian, X.F., Li, H.X., 2008. Self-assembly of active Bi_2O_3/TiO_2 visible photocatalyst with ordered mesoporous structure and highly crystallized anatase. J. Phys. Chem. C 112, 6258–6262.

Bobu, M., Wilson, S., Greibrokk, T., Lundanes, E., Siminiceanu, I., 2006. Comparison of advanced oxidation processes and identification of monuron photodegradation products in aqueous solution. Chemosphere 63, 1718–1727.

Choy, W.K., Chu, W., 2005. Destruction of o-chloroaniline in UV/TiO_2 reaction with photosensitizing additives. Ind. Eng. Chem. Res. 44, 8184–8189.

Choy, W.K., Chu, W., 2007. The use of oxyhalogen in photocatalytic reaction to remove o-chloroaniline in TiO_2 dispersion. Chemosphere 66, 2106–2113.

Chu, W., Chan, K.H., Jafvert, C.T., Chan, Y.S., 2007a. Removal of phenylurea herbicide monuron via riboflavin-mediated photo sensitization. Chemosphere 69, 177–183.

Chu, W., Choy, W.K., Kwan, C.Y., 2007b. Selection of supported cobalt substrates in the presence of oxone for the oxidation of monuron. J. Agric. Food Chem. 55, 5708–5713.

Diez, L., Livertoux, M.H., Stark, A.A., Wellman-Rousseau, M., Leroy, P., 2001. High-performance liquid chromatographic assay of hydroxyl free radical using salicylic acid hydroxylation during in vitro experiments involving thiols. J. Chromatogr. B 763, 185–193.

Eichelbe, J.W., Lichtenb, J.J., 1971. Persistence of pesticides in river water. Environ. Sci. Technol. 5, 541–544.

Elsellami, L., Vocanson, F., Dappozze, F., Puzenat, E., Paisse, O., Houas, A., Guillard, C., 2010. Kinetic of adsorption and of photocatalytic degradation of phenylalanine effect of pH and light intensity. Appl. Catal. A – Gen. 380, 142–148.

FAO, 2006. Statistical Database. <http://faostat.fao.org/> (Food and Agricultur Organization of the United Nations, Rome).

Fox, M.A., Dulay, M.T., 1993. Heterogeneous photocatalysis. Chem. Rev. 93, 341–357.

Freedman, M.L., 1960. The surface acidity of tungsten(VI) and molybdenum(VI) oxides. Anal. Chem. 32, 637–639.

Huang, Y., Zheng, Z., Ai, Z.H., Zhang, L.Z., Fan, X.X., Zou, Z.G., 2006. Core-shell microspherical Ti_1-$xZrxO_2$ solid solution photocatalysts directly from ultrasonic spray pyrolysis. J. Phys. Chem. B 110, 19323–19328.

Kim, J., Lee, C.W., Choi, W., 2010. Platinized WO_3 as an environmental photocatalyst that generates OH radicals under visible light. Environ. Sci. Technol. 44, 6849–6854.

Li, G., Lv, L., Fan, H.T., Ma, J.Y., Li, Y.Q., Wan, Y., Zhao, X.S., 2010. Effect of the agglomeration of TiO_2 nanoparticles on their photocatalytic performance in the aqueous phase. J. Colloid Interf. Sci. 348, 342–347.

Lin, J., Yu, J.C., Lo, D., Lam, S.K., 1999. Photocatalytic activity of rutile $Ti_{1-x}SnxO_2$ solid solutions. J. Catal. 183, 368–372.

Mest'ankova, H., Mailhot, G., Pilichowski, J.F., Krysa, J., Jirkovsky, J., Bolte, M., 2004. Mineralisation of monuron photoinduced by Fe(III) in aqueous solution. Chemosphere 57, 1307–1315.

Mest'ankova, H., Krysa, J., Jirkovsky, J., Mailhot, G., Bolte, M., 2005. The influence of Fe(III) speciation on supported TiO_2 efficiency: example of monuron photocatalytic degradation. Appl. Catal. B – Environ. 58, 185–191.

Mogyorosi, K., Balazs, N., Sranko, D.F., Tombacz, E., Dekany, I., Oszko, A., Sipos, P., Dombi, A., 2010. The effect of particle shape on the activity of nanocrystalline TiO_2 photocatalysts in phenol decomposition. Part 3: The importance of surface quality. Appl. Catal. B – Environ. 96, 577–585.

Nelieu, S., Shankar, M.V., Kerhoas, L., Einhorn, J., 2008. Phototransformation of monuron induced by nitrate and nitrite ions in water: contribution of photonitration. J. Photochem. Photobiol. A – Chem. 193, 1–9.

Oturan, M.A., Edelahi, M.C., Oturan, N., El Kacemi, K., Aaron, J.J., 2010. Kinetics of oxidative degradation/mineralization pathways of the phenylurea herbicides diuron, monuron and fenuron in water during application of the electro-Fenton process. Appl. Catal.B – Environ. 97, 82–89.

Pimentel, D., 1995. Amounts of pesticides reaching target pests – environmental impacts and ethics. J. Agric. Environ. Ethic 8, 17–29.

Pramauro, E., Vincenti, M., Augugliaro, V., Palmisano, L., 1993. Photocatalytic degradation of monuron in aqueous TiO_2 dispersions. Environ. Sci. Technol. 27, 1790–1795.

Ragsdale, N.N., Menzer, R.E., 1989. Carcinogenicity and Pesticides: Principles, Issues, and Relationships. American Chemical Society, Washington, DC.

Rao, Y.F., Chu, W., 2010. Linuron decomposition in aqueous semiconductor suspension under visible light irradiation with and without H_2O_2. Chem. Eng. J. 158, 181–187.

Scaife, D.E., 1980. Oxide semiconductors in photoelectrochemical conversion of solar energy. Sol. Energy 25, 41–54.

Selvam, K., Muruganandham, M., Muthuvel, I., Swaminathan, M., 2007. The influence of inorganic oxidants and metal ions on semiconductor sensitized photodegradation of 4-fluorophenol. Chem. Eng. J. 128, 51–57.

Tachikawa, T., Tojo, S., Kawai, K., Endo, M., Fujitsuka, M., Ohno, T., Nishijima, K., Miyamoto, Z., Majima, T., 2004. Photocatalytic oxidation reactivity of holes in the sulfur- and carbon-doped TiO_2 powders studied by time-resolved diffuse reflectance spectroscopy. J. Phys. Chem. B 108, 19299–19306.

Tahmasseb, L.A., Nelieu, S., Kerhoas, L., Einhorn, J., 2002. Ozonation of chlorophenylurea pesticides in water: reaction monitoring and degradation pathways. Sci. Total Environ. 291, 33–44.

USEPA (United States Environmental Protection Agency), 2004. Exposure and Human Health Reassessment of 2,3,7,8-Tetrachlorodibenzo-p-Dioxin (TCDD) and Related Compounds National Academy Sciences (NAS) Review Draft. Part I, vol. 1 (Chapter 8), Washington, DC.

Wang, Y.B., Hong, C.S., 1999. Effect of hydrogen peroxide, periodate and persulfate on photocatalysis of 2-chlorobiphenyl in aqueous TiO_2 suspensions. Water Res. 33, 2031–2036.

Yang, H.M., Shi, R.R., Zhang, K., Hu, Y.H., Tang, A.D., Li, X.W., 2005. Synthesis of WO_3/TiO_2 nanocomposites via sol–gel method. J. Alloy. Compd. 398, 200–202.

Zaleska, A., Sobczak, J.W., Grabowska, E., Hupka, J., 2008. Preparation and photocatalytic activity of boron-modified TiO_2 under UV and visible light. Appl. Catal. B – Environ. 78, 92–100.